



Triclosan inhibits the activation of human periodontal ligament fibroblasts induced by lipopolysaccharide from *Porphyromonas gingivalis*

Wei Shu^{1,2,Δ}, Yanman Zhang^{1,Δ}, Chen Zhang³, Qiang You³, Hong Zhou^{1,3,✉}, Shuang Wen^{1,✉}

¹Department of Immunology, School of Basic Medical Sciences, Nanjing Medical University, Nanjing, Jiangsu 211166, China;

²Department of Stomatology, Jiangsu Provincial Hospital of Traditional Chinese Medicine, Nanjing, Jiangsu 210029, China;

³Department of Biotherapeutics, the Second Affiliated Hospital of Nanjing Medical University, Nanjing, Jiangsu 210011, China.

Abstract

Periodontitis is a highly prevalent, chronic, non-specific, and immunologically devastating disease of periodontal tissues, caused by microbial infection. This study aims to examine the efficacy and protective mechanism of triclosan (TCS), a bisphenolic, non-cationic component of oral care products, against periodontal inflammation induced by lipopolysaccharide purified from *Porphyromonas gingivalis* (LPS-PG). TCS markedly downregulated interleukin-6 (IL-6), IL-8, and IL-15 in human periodontal ligament fibroblasts (HPDLFs) treated with LPS-PG. By using a liquid chromatography-tandem mass spectrometry (LC-MS/MS) approach, 318 differentially expressed proteins (161 upregulated and 157 downregulated) were identified in TCS-pretreated HPDLFs. TCS upregulated HSPA5 and HSP90B1 but downregulated HSPA2. Besides, TCS upregulated miR-548i in HPDLFs, which downregulated IL-15. These results indicate that TCS attenuates the activation of HPDLFs and downregulates the inflammatory cytokines through various mechanisms, thus highlighting its protective role in periodontal inflammation.

Keywords: human periodontal ligament fibroblasts, lipopolysaccharide, triclosan, heat shock protein

Introduction

Periodontitis is a common oral disease and is the predominant cause of tooth loss in adults. Pathogen-induced activation of periodontal resident cells causes chronic periodontal inflammation, leading to local ischemia and inflammatory cell infiltration, eventually resulting in tissue necrosis^[1-2]. Periodontitis

progression may cause chronic periodontal destruction and even the loosening or loss of teeth^[3]. Furthermore, various inflammatory cytokines produced during periodontal inflammation can reach other organs through blood circulation and are thus speculated to be associated with other diseases^[4-7]. However, therapeutic strategies for chronic periodontal inflammation are relatively limited and ineffective^[8].

^ΔThese authors contributed equally to this work.

[✉]Corresponding authors: Shuang Wen and Hong Zhou, Department of Immunology, School of Basic Medical Sciences, Nanjing Medical University, 101 Longmian Avenue, Nanjing, Jiangsu 211166, China. Tel: +86-25-86869456, E-mails: swen@njmu.edu.cn and hongzhou@live.com.

Received: 21 February 2020; Revised: 24 June 2020; Accepted: 30 June 2020; Published online: 31 August 2020

© 2021 by the Journal of Biomedical Research.

CLC number: R781.4, Document code: A

The authors reported no conflict of interests.

This is an open access article under the Creative Commons Attribution (CC BY 4.0) license, which permits others to distribute, remix, adapt and build upon this work, for commercial use, provided the original work is properly cited.

Human periodontal ligament fibroblasts (HPDLFs), similar to gingival fibroblasts, synthesize the collagen present in and supporting the periodontal tissues^[9–10]. When activated by components of exogenous pathogens, *e.g.*, lipopolysaccharides of *Porphyromonas gingivalis* (LPS-PG), HPDLFs produce various pro-inflammatory cytokines and chemokines, including interleukin-6 (IL-6), IL-8, and IL-15, further promoting the immune responses and exacerbating periodontal tissue damage^[11–12]. The concomitant chronic periodontitis activates immune cells and induces them to produce various cytokines that aggravate periodontal tissue damage^[13–15]. Without timely treatment, destruction to periodontal tissue, root exposure, tooth loosening, and tooth loss can occur^[16]. Blockade of the periodontal fibroblast activation mitigates the destruction of periodontal tissue, serving as a key strategy for treating chronic periodontal inflammation^[17].

Triclosan (TCS) is a bisphenolic and non-cationic agent used in oral care products owing to its broad-spectrum anti-microbial and anti-plaque activity^[18]. Incorporation of a TCS-based monomer into the resin matrix of dental composites reduces the bacterial adhesion of *Streptococcus mutans* without affecting important polymer properties, thus improving the long-term performance of these restorative materials^[19]. TCS also reduces the microbial load during the pathogenesis of gingivitis^[20]. Compared to conventional fluoride dentifrice, it effectively controls plaque formation and prevents or alleviates gingivitis^[21–23]. However, the detailed mechanism underlying the potential inhibitory effects of TCS on periodontal inflammation remains unclear.

In this study, we sought to elucidate the effects of TCS on LPS-PG-induced activation of periodontal fibroblasts. With liquid chromatography-tandem mass spectrometry (LC-MS/MS) and transcriptome array, we investigated the differentially expressed proteins and determined the pathways mediating the protective effects of TCS against periodontitis.

Material and methods

Reagents

LPS-PG was purchased from InvivoGen (USA). TCS was purchased from Sigma-Aldrich (USA). Enzyme-linked immunosorbent assay (ELISA) kits for IL-6, IL-8, and IL-15 were purchased from eBioscience (USA). Anti-IL-15 and anti- β -actin antibodies were purchased from Abcam Biotechnology (USA). Lipofectamine 3000 was purchased from Invitrogen (USA). The cell counting kit-8 (CCK-8)

reagent was purchased from Dojindo Laboratories (Japan). Enhanced chemiluminescence reagents were purchased from PerkinElmer (USA). The miR-548i overexpression vector and inhibitors were purchased from GenePharma (China). HPDLFs (Cat. No.: XY2630) were purchased from the Shanghai Xinyu Biological Company (China).

Cell culture and treatment

HPDLFs are immortalized cells, capable of displaying positive staining for vimentin and negative staining for keratin. They extend to a spindle shape upon adherence to the substratum. HPDLFs were cultured in high-glucose Dulbecco's modified Eagle's medium (DMEM) supplemented with 10% fetal bovine serum (Thermo Fisher Scientific, USA) and 1% penicillin/streptomycin solution (100 U/mL penicillin and 100 μ g/mL streptomycin). Cells were seeded in six-well plates at 50% confluence in complete medium supplemented with 10% FBS and incubated at 37 °C for 24 hours with 5% CO₂. The medium was changed to a serum-free medium for another 16 hours, and then pretreated with TCS at 0 or 1 μ g/mL for 2 hours and then treated with 100 ng/mL LPS-PG for 24 hours.

CCK-8 assay

A total of 2×10^3 HPDLFs were seeded in 96-well plates and pretreated with TCS at various concentrations (0, 0.25, 0.5, 0.75, 1, 2 or 5 μ g/mL) for 2 hours, and then LPS-PG (0 or 100 ng/mL) was added to the medium for 24 hours. Thereafter, 10 μ L of CCK-8 solution was added to each well, and the plate was incubated at 37 °C for 2 hours with 5% CO₂. Cell proliferation was assessed following the manufacturer's instructions, and the optical density of each well was measured at 450 nm using a microplate reader (Bio-Tek ELX800, USA).

qRT-PCR analysis

LPS-PG-stimulated HPDLFs were homogenized in Trizol (Thermo Fisher Scientific) under the manufacturer's instructions to obtain total RNA, which was then reverse-transcribed into cDNA. SYBR green-based qRT-PCR analysis was performed for IL-6 and IL-8 using StepOnePlus (Thermo Fisher Scientific). The amplification conditions were as follows: 95 °C (1 minute) followed by 35 cycles of 95 °C (10 seconds), 60 °C (30 seconds), and 95 °C (15 seconds). Expression levels of target genes were normalized to those of *GAPDH* as the internal control. Primer sequences are provided in **Supplementary Table 1** (available online). Each sample was analyzed

in triplicate, and changes in the relative expression were determined using the comparative Ct method.

Quantification of the inflammatory cytokines IL-6, IL-8, and IL-15

TCS-pretreated, LPS-PG-stimulated HPDLFs were centrifuged at 5000 g for 10 minutes, and the supernatant was harvested to quantify the inflammatory cytokines IL-6, IL-8, and IL-15 using ELISA kits as per the manufacturer's instructions.

LC-MS/MS analysis

Proteins extracted from the TCS intervention group and the LPS-PG-induced inflammation group were digested and subsequently analyzed using a Triple-TOF 5600+ mass spectrometer (AB Sciex, USA). A capillary RP-LC column (75 μm i.d. \times 150 mm, filled with Acclaim PepMap RSLC C18, 100 \AA , 2 μm , nanoViper Dionex, USA) was used to separate peptides through LC. Samples were desalted from the autosampler at 5 $\mu\text{L}/\text{minute}$ by loading them onto a trap column (Acclaim PepMap 100 C18, 100 \AA , 3 μm , 75 μm \times 2 cm, Dionex). The desalted samples were then washed for 12 minutes with 0.1% FA in HPLC-grade water, and the system was adjusted to line up with the analytical RP capillary column. The tryptic digest was analyzed within 65 minutes with a three-step gradient (80% ACN in 0.1% methanol from 4% to 50% over 45 minutes, 50% to 90% over 5 minutes, and at 95% for 15 minutes) at a flow rate of 300 nL/minute.

Bioinformatics analysis of proteomics data

All proteins with significant differences in abundance between the LPS-PG and LPS-PG+TCS groups were analyzed by Gene Ontology (GO) terms for biological process, cellular component, and molecular function using the Software Tool for Rapid Annotation of Proteins (STRAP). Pathway enrichment analysis of protein clusters was assessed in accordance with the Kyoto Encyclopedia of Genes and Genomes (KEGG) pathway database. Protein-protein interactions (PPI) were analyzed using the Search Tool for the Retrieval of Interacting Genes/Proteins version 10 (STRING) database.

Western blotting analysis

Cultured HPDLFs were lysed in RIPA lysis buffer (Beyotime, China) on ice for 30 minutes. Supernatants were harvested through centrifugation at 13 000 g and 4 $^{\circ}\text{C}$ for 30 minutes. Protein samples were homogenized with loading buffer and heated to 100 $^{\circ}\text{C}$ for 5 minutes, and 20 μg of each sample was then resolved through SDS-PAGE (10% resolving gel). Proteins

were transferred to polyvinylidene difluoride membranes (Millipore, USA). The membranes were blocked with 5% dry milk for 1 hour at 25 $^{\circ}\text{C}$ and incubated with primary anti-IL-15 (1:1000 dilution) and anti- β -actin (1:1000 dilution) antibodies overnight at 4 $^{\circ}\text{C}$. The membranes were washed and incubated in horseradish peroxidase-conjugated secondary antibody (1:10 000 dilution) for 2 hours at room temperature. Protein levels were determined using enhanced chemiluminescence reagents and quantified using ImageJ software (NIH, Bethesda, USA).

miRNA transfection

HPDLFs were cultured in six-well plates up to 70% confluence. Cells were transfected with Lipofectamine 3000 as per the manufacturer's instructions. Briefly, 5 μL of miR-548i mimics or inhibitors, and 6 μL of Lipofectamine 3000 were diluted in 250 μL of Opti-MEM reduced serum medium (Thermo Fisher Scientific), and then diluted Lipofectamine 3000 was added into the mimics or inhibitors. The mixture was incubated at room temperature for 15 minutes and then added to the cell culture medium. The cultured cells were then incubated at 37 $^{\circ}\text{C}$ for 36 hours. Green fluorescence was observed under the microscope to determine whether transfection was successful and if the vector was expressed.

Transcriptome array analysis

First-strand cDNA was synthesized using the "First-Strand cDNA Synthesis" program, and the second-strand cDNA was synthesized using the "Second-Strand cDNA Synthesis" program. The cRNA was purified using the WT PLUS Reagent Kit (Thermo Fisher Scientific), and its concentration was determined. cRNA and 2nd-Cycle Primers Mix were prepared and incubated with the "2nd-Cycle Primers-cRNA Annealing" program; 2nd-Cycle ss-cDNA Master Mix was prepared and incubated using the "2nd-Cycle ss-cDNA Synthesis" program for the second cycle of single-stranded cDNA synthesis. Thereafter, RNA was hydrolyzed with RNase H using the "RNA Hydrolysis" program; the single-stranded cDNA of the second cycle was purified using the WT PLUS Kit, and the concentration was measured. Further, the "Fragmentation" and "Labeling" programs were used to fragment and label cDNA. Hybridization experiments were then carried out, and the GeneChip Fluidics Station 450 (Affymetrix, USA) instrument was used for automatic washing and dyeing. Scanning was performed after dyeing to obtain the data.

Statistical analysis

Data were analyzed using SPSS 17 software (17.0

for Windows, IBM, USA). All data are expressed as mean±SD values and were analyzed using unpaired two-tailed Student's *t*-test for two treatment groups and one-way ANOVA followed by Bonferroni's post-hoc multiple comparisons test for multiple treatment groups. Significant differences in gene/protein expression levels were considered when $P < 0.05$.

Results

TCS pretreatment downregulated IL-6, IL-8, and IL-15 induced by LPS-PG in HPDLFs

First, we examined whether TCS affected the viability of HPDLFs at various concentrations, through CCK-8 assays. At a concentration of ≤ 1 $\mu\text{g/mL}$, TCS was nontoxic to HPDLFs; however, 2 and 5 $\mu\text{g/mL}$ TCS affected the HPDLFs viability (**Fig. 1A**). Therefore, the concentration of TCS at 1 $\mu\text{g/mL}$ was used in the subsequent experiments. To further investigate the effect of TCS on the oral inflammatory response, we generated an *in vitro* model of periodontal inflammation by treating HPDLFs with LPS-PG. LPS-PG treatment upregulated the inflammatory cytokines (*IL6*, *IL8*, and *IL15*) in HPDLFs, while pretreatment of HPDLFs with 1 $\mu\text{g/mL}$ TCS significantly inhibited the

production of these inflammatory cytokines (**Fig. 1B**). However, on the initially established inflammatory model, the inhibitory capabilities of 1 $\mu\text{g/mL}$ of TCS after TCS treatment were found not as effective as those during pretreatment (**Supplementary Fig. 1**, available online). Besides, qRT-PCR analysis also revealed that TCS at a concentration of 1 $\mu\text{g/mL}$ significantly suppressed these cytokines in HPDLFs (**Fig. 1C**). Therefore, TCS suppressed the activation of HPDLFs induced by LPS-PG.

LC-MS/MS analysis and pathway enrichment analysis of differentially expressed proteins in HPDLFs pretreated with TCS or treated with LPS-PG alone

To investigate the mechanism through which TCS inhibits the LPS-PG-induced activation of HPDLFs, LC-MS/MS analysis was performed on the extracts of HPDLFs treated with TCS and LPS-PG, or LPS-PG alone. Hierarchical cluster analysis indicated that 318 significantly differentially expressed proteins were obtained in TCS-pretreated HPDLFs, compared to those treated only with LPS-PG. These proteins include 161 upregulated and 157 downregulated proteins (**Fig. 2A**). The pathways involving these differentially expressed proteins were further analyzed and screened using KEGG database, and they were

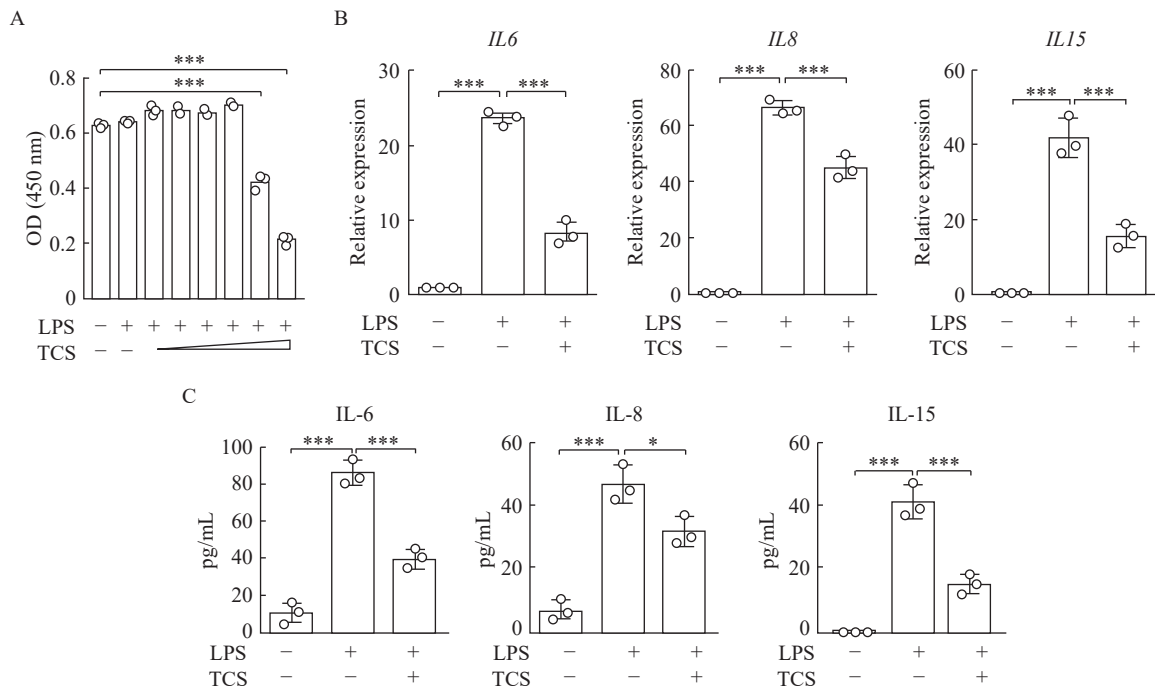


Fig. 1 TCS decreased the mRNA and protein levels of inflammatory cytokines in activated HPDLFs. A: HPDLFs were pretreated with TCS at concentrations of 0–5 $\mu\text{g/mL}$; then, LPS-PG (100 ng/mL) was added to the culture for 24 hours. Cell viability was examined using cell counting kit-8 assays. B: HPDLFs were pretreated with TCS at a concentration of 1 $\mu\text{g/mL}$, and mRNA levels of *IL6*, *IL8*, and *IL15* in HPDLFs were quantified using qRT-PCR. C: HPDLFs were pretreated with TCS at a concentration of 1 $\mu\text{g/mL}$, and protein levels of IL-6, IL-8, and IL-15 in the culture were measured using enzyme-linked immunosorbent assays. Data are presented as mean±SD and were analyzed using unpaired two-tailed Student's *t*-test. * $P < 0.05$, ** $P < 0.01$, *** $P < 0.001$, $n = 3$.

found to be enriched in ribosomal function, protein processing, antigen processing and presentation, and phagocytic function, among other pathways (**Fig. 2B**).

Gene ontology analysis of differentially expressed proteins in HPDLFs pretreated with TCS or treated with LPS-PG alone

The differentially expressed proteins were then submitted as an input into the GO database for functional analysis. During GO enrichment analysis of the up-regulated proteins using the STRAP classification for biological processes, they were primarily enriched during translational initiation; for cellular components, they were significantly enriched in extracellular exosomes and extracellular matrix; for molecular function, they were enriched in protein binding (**Fig. 3A**). During GO enrichment analysis of the down-regulated proteins using the STRAP classification for biological processes, they were significantly enriched during translational initiation; for cellular component, they were significantly enriched in extracellular exosome and extracellular matrix; for molecular function, they were enriched in protein binding and unfolded protein binding (**Fig. 3B**). Therefore, TCS significantly affected the biological response of HPDLFs treated with LPS-PG by affecting translational initiation, formation of extracellular exosomes, and protein binding.

Protein-protein interaction analysis of differentially expressed proteins in HPDLFs pretreated with TCS or treated with LPS-PG alone

The STRING database was used to analyze the potential interactions among differentially expressed proteins, and 35 key proteins were involved in a PPI network. Several proteins played a key role in the obtained PPI network and were screened as candidate proteins. Among upregulated proteins, HSPA5 was strongly associated with HSP90B1 and human leukocyte antigen-A (HLA-A) (**Fig. 4A**). Among downregulated proteins, ATP-citrate lyase (ACLY) was closely associated with hexosaminidase B (HEXB) and peroxiredoxin-6 (PRDX6) (**Fig. 4A**). Based on the significant GO enrichment, pathway enrichment, and PPI analysis, key molecules involved in the inflammatory signaling pathway of LPS-PG-treated HPDLFs pretreated with TCS were screened. Hierarchical cluster analysis indicated that five candidate proteins, HSPA2, HLA-A, PD1A4, HSPA5, and HSP90B1, were differentially expressed in TCS-pretreated HPDLFs (**Fig. 4B**). On importing these proteins into the STRING database, IL-6 and IL-8 expression levels were found to be associated with HSPA5 and HSP90B1 (**Fig. 4C**). These results indicated that IL-6 and IL-8 expression was potentially associated with HSPA5 and HSP90B1 in LPS-PG-treated HPDLFs.

TCS upregulated miR-548i and downregulated IL-15 in HPDLFs

Few proteins displayed TCS-altered expression; therefore, we used a transcriptome array to further examine the mRNA expression levels of inflammatory

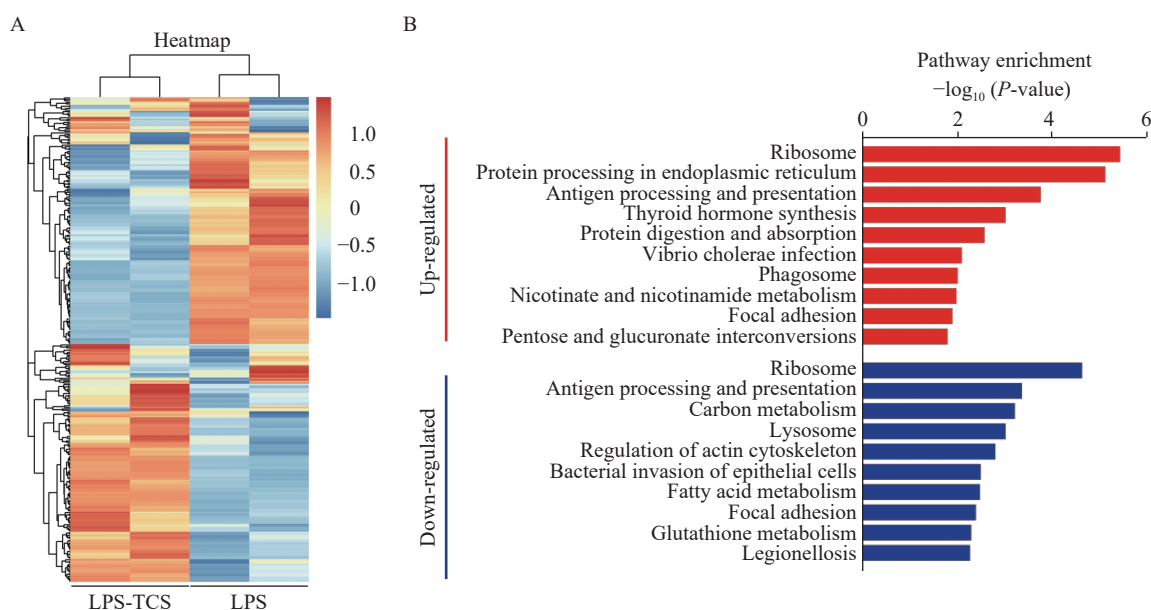


Fig. 2 LC-MS/MS analysis and pathway enrichment analysis of differentially expressed proteins in HPDLFs pretreated with TCS or treated with LPS-PG alone. HPDLFs were pretreated with TCS and then treated with LPS-PG for 24 hours. A: Hierarchical cluster analysis of 318 differentially expressed proteins. B: The top ten significantly up- or downregulated pathways based on the KEGG database.

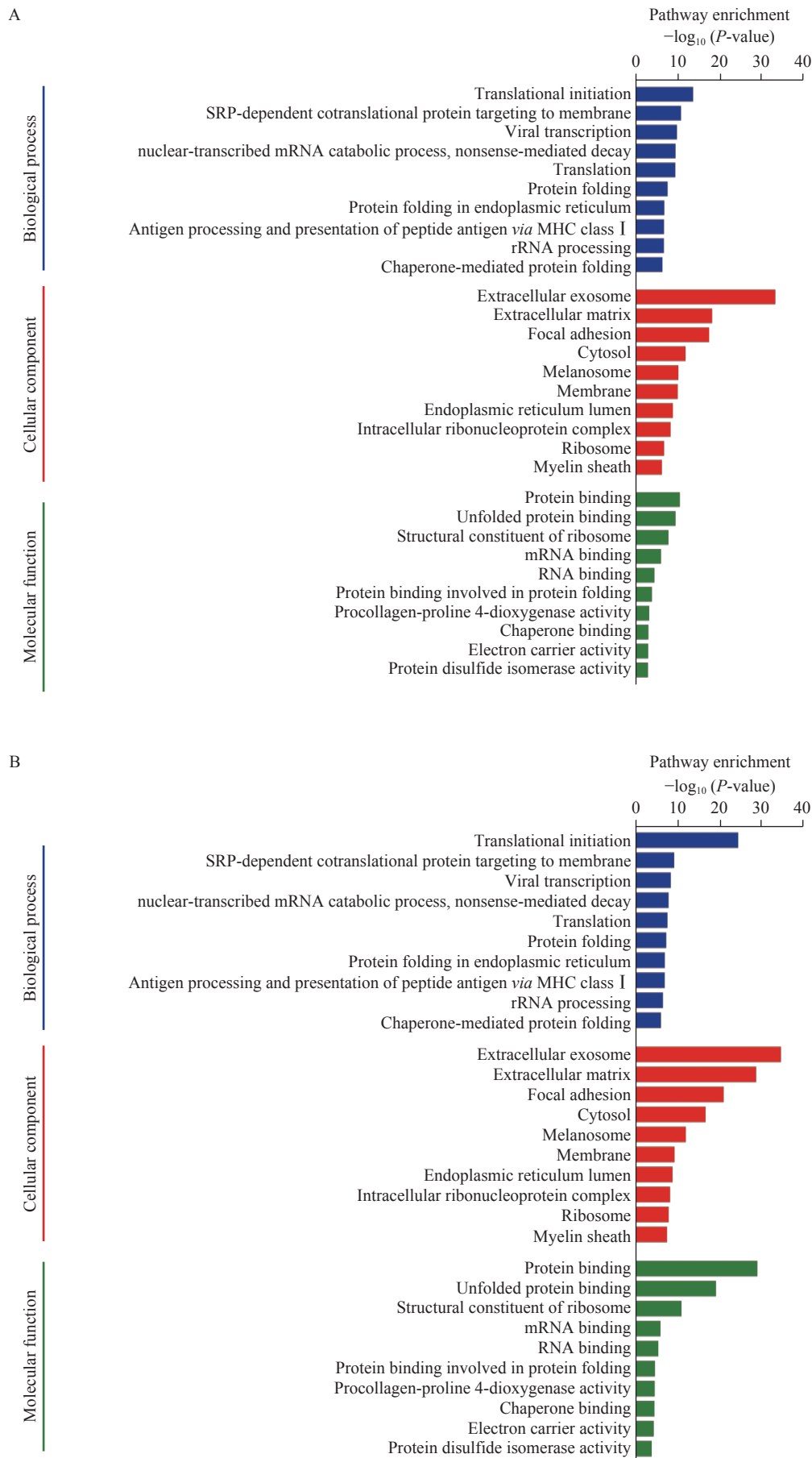


Fig. 3 Gene ontology analysis of differentially expressed proteins in HPDLFs pretreated with TCS or treated with LPS-PG alone. Top 10 significantly upregulated (A) and downregulated (B) differentially expressed proteins in biological processes, cellular components, and molecular functions in HPDLFs pretreated with TCS and then exposed to LPS-PG.

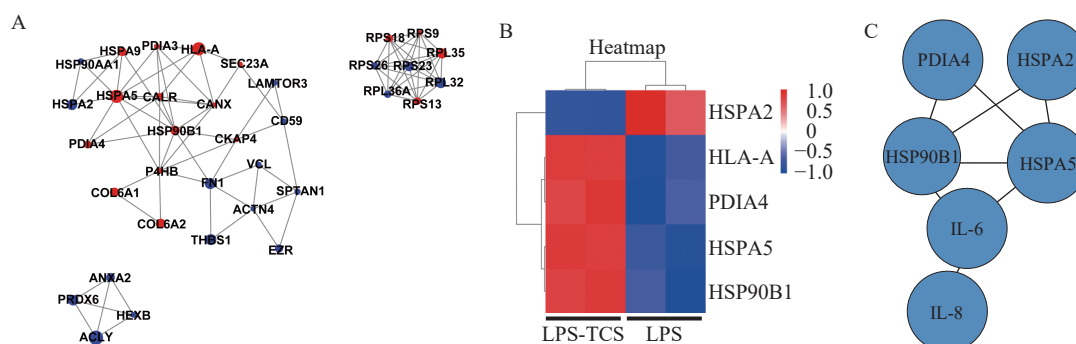


Fig. 4 Protein-protein interaction analysis of differentially expressed proteins in HPDLFs pretreated with TCS or treated with LPS-PG alone. A: PPI network of differentially expressed proteins in HPDLFs pretreated with TCS or treated with LPS-PG alone. Red and blue circles represent upregulated and downregulated proteins, respectively. The larger the area of the circle, the higher the degree of difference. B: Hierarchical cluster analysis of five candidate proteins involved in the inflammatory response of HPDLFs pretreated with TCS and then treated with LPS-PG. C: PPI network of the five candidate proteins based on STRING. PPI: protein-protein interactions; STRING: Search Tool for the Retrieval of Interacting Genes/Proteins.

cytokines in HPDLFs treated either with LPS-PG alone or both LPS-PG and TCS. A significant positive correlation was obtained for mRNA expression with respect to both the LPS-PG-induced and TCS intervention groups (**Fig. 5A**). For each gene, the signal strength distribution between TCS intervention group and the LPS-PG-induced inflammation group could be visualized using a scatter plot (**Fig. 5B**). Furthermore, 49 differentially expressed genes with a fold change value of >1.5 were identified (**Fig. 5C**), among which miR-548i was the most significant differentially expressed gene. qRT-PCR analysis confirmed miR-548i upregulation in TCS-treated HPDLFs (**Fig. 6A**). Target scan predictions suggest that IL-15 expression might be regulated by miR-548i. In the miR-548i overexpression system (**Fig. 6B**), treatment with TCS in the presence of LPS-PG downregulated *IL15* in comparison with LPS-PG treatment alone at mRNA (**Fig. 6C**) and protein (**Fig. 6E**) levels. In the miR-548i inhibition system, TCS treatment did not influence *IL15* levels in comparison with LPS-PG treatment alone at mRNA (**Fig. 6D**) and protein (**Fig. 6F**) levels. Furthermore, treatment with TCS in the presence of LPS-PG downregulated IL-6 and IL-8 in comparison with LPS-PG treatment alone at mRNA level in the miR-548i overexpression system but didn't change in the miR-548i inhibition system (**Supplementary Fig. 2A and B**, available online).

Discussion

TCS has recently been implicated in the pathogenesis and progression of numerous diseases. This study shows that TCS significantly downregulates the LPS-PG-induced expression of the inflammatory factors IL-6, IL-8, and IL-15, attenuating the activation of HPDLFs, thus potentially

inhibiting bacterial infection induced periodontitis.

In inflammatory responses, heat shock proteins (HSPs) can be upregulated by various stressors, including oxidative and endoplasmic reticulum stress^[24]. Herein, TCS treatment significantly upregulated multiple HSP molecules; for instance, HSPA2 was upregulated, while HSPA5 and HSP90B1 were downregulated along with IL-6. TCS reportedly reduces liver HSP90 levels^[25]. We speculated that these HSPs may participate in the activation of HPDLFs and are potentially suppressed by TCS. However, these HSPs potentially do not regulate the expression of inflammatory cytokines in LPS-PG treated HPDLFs because they seldom exert any biological effects on the expression of inflammatory genes. Further studies are required to elucidate the role of HSPA5 and HSP90B1 in LPS-PG-induced HPDLF activation.

Interestingly, at the mRNA level, both LPS-PG and TCS treatment upregulated miR-548i. However, LPS-PG was expected to upregulate certain miRNAs. Furthermore, miR-548i overexpression significantly downregulated IL-15 in HPDLFs, suggesting the upregulation of miR-548i might inhibit the expression of IL-15 in TCS treated cells. However, the potential involvement of other non-coding RNAs in the regulation and expression of other inflammatory cytokines cannot be ruled out. Furthermore, the detailed mechanisms underlying the association between miR-548i and IL-15 production require further investigation.

In summary, this is the first study, to our knowledge, to show that TCS could significantly reduce the LPS-PG-induced production of inflammatory factors IL-6, IL-8, and IL-15 in HPDLFs, and thus attenuate the activation of HPDLFs, indicating that TCS could potentially protect against periodontal inflammation.

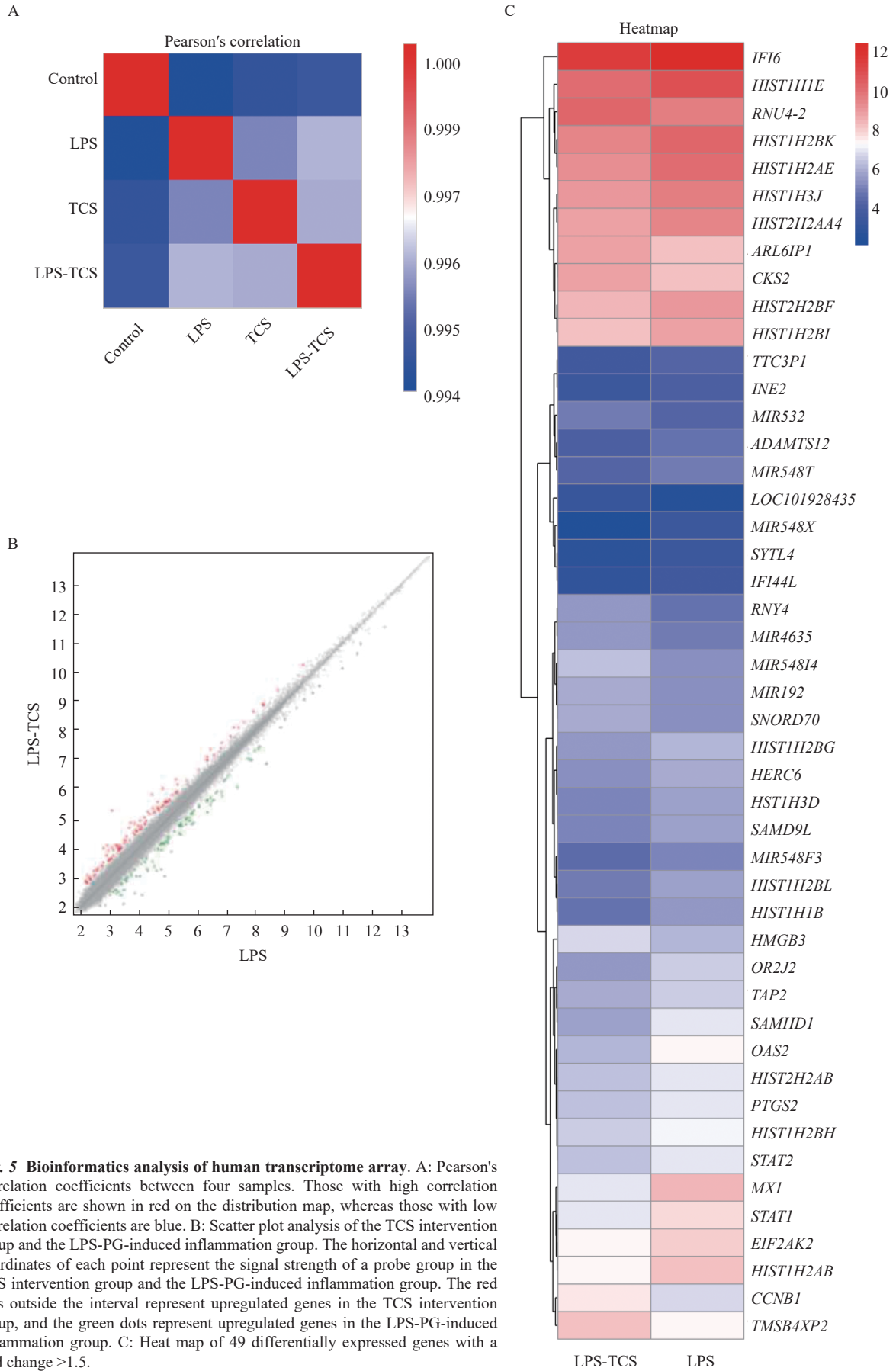


Fig. 5 Bioinformatics analysis of human transcriptome array. A: Pearson's correlation coefficients between four samples. Those with high correlation coefficients are shown in red on the distribution map, whereas those with low correlation coefficients are blue. B: Scatter plot analysis of the TCS intervention group and the LPS-PG-induced inflammation group. The horizontal and vertical coordinates of each point represent the signal strength of a probe group in the TCS intervention group and the LPS-PG-induced inflammation group. The red dots outside the interval represent upregulated genes in the TCS intervention group, and the green dots represent upregulated genes in the LPS-PG-induced inflammation group. C: Heat map of 49 differentially expressed genes with a fold change >1.5.

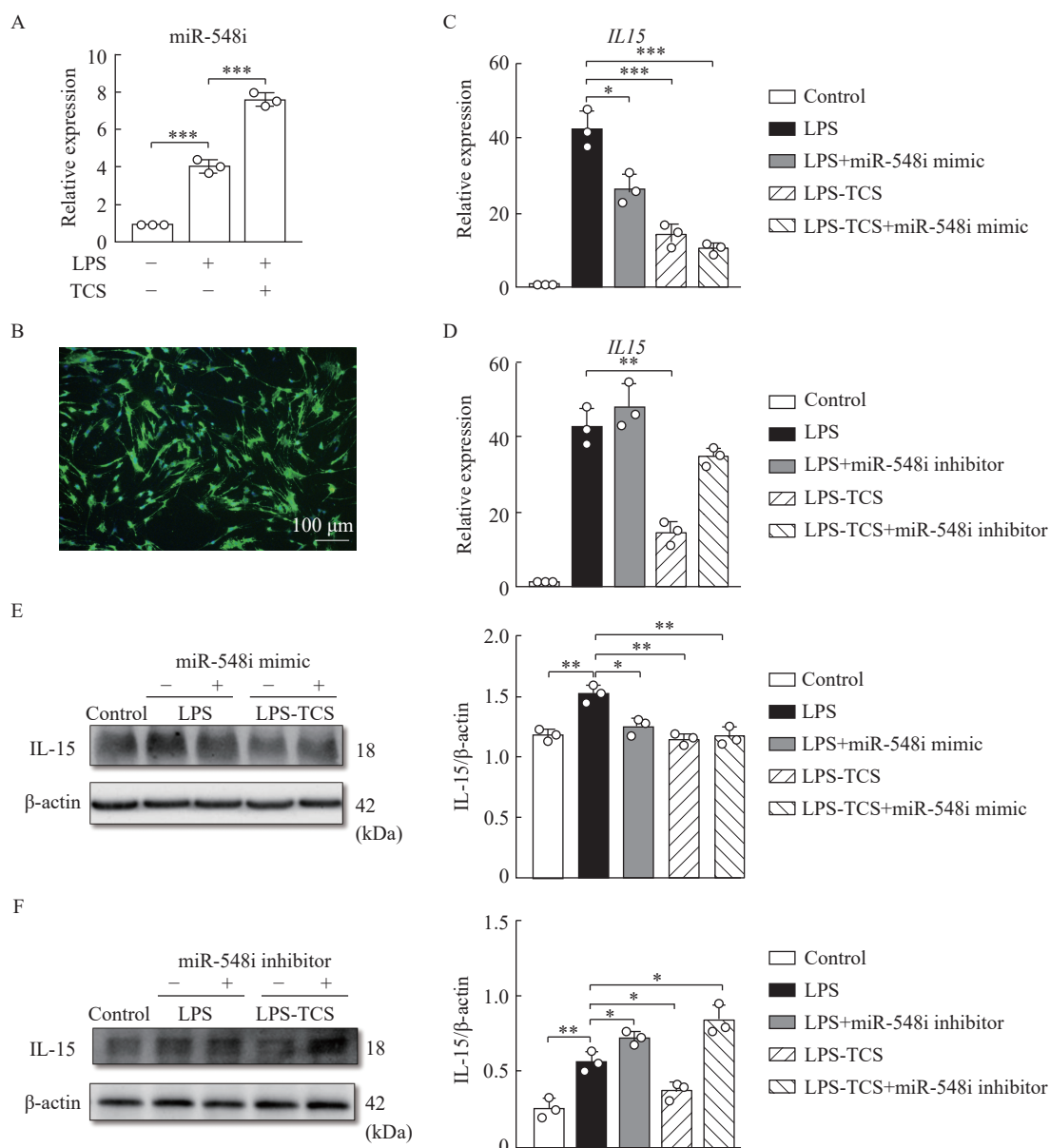


Fig. 6 Role of miR-548i in TCS-treated HPDLFs. HPDLFs were transfected with either miR-548i mimics or inhibitors. A: qRT-PCR analysis of the relative expression of miR-548i expression in the TCS intervention and the LPS-PG inflammation groups. B: Transfection efficiency of miR-548i mimics. HPDLFs were probed with DAPI (blue) and miR-548i mimics (green). C and D: mRNA levels of *IL15* in the miR-548i overexpression system and inhibition system. E and F: IL-15 protein levels in the miR-548i overexpression and inhibition system were detected by Western blotting. The left panel shows western blotting images, and the right panel denotes the quantitative findings. Data are presented as mean \pm SD and were analyzed using unpaired two-tailed Student's *t*-test. *** P <0.001, n =3.

Acknowledgments

This work was funded by the innovative development funds of Jiangsu Province Hospital of Traditional Chinese Medicine (Y2018CX19).

References

- [1] Scully C, Epstein J, Sonis S. Oral mucositis: a challenging complication of radiotherapy, chemotherapy, and radiochemotherapy. Part 2: diagnosis and management of mucositis[J]. *Head Neck*, 2004, 26(1): 77–84.
- [2] Kinane DF, Stathopoulou PG, Papapanou PN. Periodontal diseases[J]. *Nat Rev Dis Primers*, 2017, 3(1): 17038.
- [3] Dopico J, Nibali L, Donos N. Disease progression in aggressive periodontitis patients. A retrospective study[J]. *J Clin Periodontol*, 2016, 43(6): 531–537.
- [4] Otomo-Corgel J, Pucher JJ, Rethman MP, et al. State of the science: chronic periodontitis and systemic health[J]. *J Evid Based Dent Pract*, 2012, 12(3S): 20–28.
- [5] Manjunath BC, Praveen K, Chandrashekar BR, et al. Periodontal infections: a risk factor for various systemic diseases[J]. *Natl Med J India*, 2011, 24(4): 214–219.

- [6] Gotsman I, Lotan C, Soskolne WA, et al. Periodontal destruction is associated with coronary artery disease and periodontal infection with acute coronary syndrome[J]. *J Periodontol*, 2007, 78(5): 849–858.
- [7] Kaisare S, Rao J, Dubashi N. Periodontal disease as a risk factor for acute myocardial infarction. A case-control study in Goans highlighting a review of the literature[J]. *Br Dent J*, 2007, 203(3): E5.
- [8] Graves DT, Li J, Cochran DL. Inflammation and uncoupling as mechanisms of periodontal bone loss[J]. *J Dent Res*, 2011, 90(2): 143–153.
- [9] Kim BC, Song JI, So KH, et al. Effects of lysophosphatidic acid on human periodontal ligament stem cells from teeth extracted from dental patients[J]. *J Biomed Res*, 2019, 33(2): 122–130.
- [10] Wei FL, Wang CL, Zhou GY, et al. The effect of centrifugal force on the mRNA and protein levels of ATF4 in cultured human periodontal ligament fibroblasts[J]. *Arch Oral Biol*, 2008, 53(1): 35–43.
- [11] Sweier DG, Shelburne PS, Giannobile WV, et al. Immunoglobulin G (IgG) class, but not IgA or IgM, antibodies to peptides of the *Porphyromonas gingivalis* chaperone HtpG predict health in subjects with periodontitis by a fluorescence enzyme-linked immunosorbent assay[J]. *Clin Vaccine Immunol*, 2009, 16(12): 1766–1773.
- [12] Morandini AC, Chaves Souza PP, Ramos-Junior ES, et al. MyD88 or TRAM knockdown regulates interleukin (IL)-6, IL-8, and CXCL12 mRNA expression in human gingival and periodontal ligament fibroblasts[J]. *J Periodontol*, 2013, 84(9): 1353–1360.
- [13] Paster BJ, Olsen I, Aas JA, et al. The breadth of bacterial diversity in the human periodontal pocket and other oral sites[J]. *Periodontology 2000*, 2006, 42(1): 80–87.
- [14] Bostanci N, Belibasakis GN. *Porphyromonas gingivalis*: an invasive and evasive opportunistic oral pathogen[J]. *FEMS Microbiol Lett*, 2012, 333(1): 1–9.
- [15] Terheyden H, Stadlinger B, Sanz M, et al. Inflammatory reaction – communication of cells[J]. *Clin Oral Implants Res*, 2014, 25(4): 399–407.
- [16] Ley C, Sundaram V, de la Luz Sanchez M, et al. Triclosan and triclocarban exposure, infectious disease symptoms and antibiotic prescription in infants – a community-based randomized intervention[J]. *PLoS One*, 2018, 13(6): e0199298.
- [17] Rodricks JV, Swenberg JA, Borzelleca JF, et al. Triclosan: a critical review of the experimental data and development of margins of safety for consumer products[J]. *Crit Rev Toxicol*, 2010, 40(5): 422–484.
- [18] Geens T, Neels H, Covaci A. Distribution of bisphenol-A, triclosan and n-nonylphenol in human adipose tissue, liver and brain[J]. *Chemosphere*, 2012, 87(7): 796–802.
- [19] Azzouz A, Rascón AJ, Ballesteros E. Simultaneous determination of parabens, alkylphenols, phenylphenols, bisphenol A and triclosan in human urine, blood and breast milk by continuous solid-phase extraction and gas chromatography-mass spectrometry[J]. *J Pharm Biomed Anal*, 2016, 119: 16–26.
- [20] Pancer BA, Kott D, Sugai JV, et al. Effects of triclosan on host response and microbial biomarkers during experimental gingivitis[J]. *J Clin Periodontol*, 2016, 43(5): 435–444.
- [21] Blinkhorn A, Bartold PM, Cullinan MP, et al. Is there a role for triclosan/copolymer toothpaste in the management of periodontal disease?[J]. *Br Dent J*, 2009, 207(3): 117–125.
- [22] Sälzer S, Slot DE, Dörfer CE, et al. Comparison of triclosan and stannous fluoride dentifrices on parameters of gingival inflammation and plaque scores: a systematic review and meta-analysis[J]. *Int J Dent Hyg*, 2015, 13(1): 1–17.
- [23] Valkenburg C, Else Slot D, Van der Weijden GA. What is the effect of active ingredients in dentifrice on inhibiting the regrowth of overnight plaque? A systematic review[J]. *Int J Dent Hyg*, 2020, 18(2): 128–141.
- [24] Zheng XB, Xu F, Liang H, et al. SIRT1/HSF1/HSP pathway is essential for exenatide-alleviated, lipid-induced hepatic endoplasmic reticulum stress[J]. *Hepatology*, 2017, 66(3): 809–824.
- [25] Wang CH, Huang WH, Lin JB, et al. Triclosan-induced liver and brain injury in zebrafish (*Danio rerio*) via abnormal expression of miR-125 regulated by PKC α /Nrf2/p53 signaling pathways[J]. *Chemosphere*, 2020, 241: 125086.